Agenzia nazionale per le nuove tecnologie,
l'energia e lo sviluppo economico sostenibile

MINISTERO DELLO SVILUPPO ECONOMICO

Pre-test CFD analysis of the Blockage Fuel Pin Simulator (BFPS) test section for the NACIE-UP facility

Ivan Di Piazza, Ranieri Marinari

Report RdS/PAR2015/033

PRE-TEST CFD ANALYSIS OF THE BLOCKAGE FUEL PIN SIMULATOR (BFPS) TEST SECTION FOR THE NACIE-UP FACILITY

Ivan Di Piazza (ENEA), Ranieri Marinari (UNIPI)

Settembre 2016

Report Ricerca di Sistema Elettrico

Accordo di Programma Ministero dello Sviluppo Economico - ENEA
Piano Annuale di Realizzazione 2015
Area: Generazione di Energia Elettrica con Basse Emissioni di Carbonio
Progetto: Sviluppo competenze scientifiche nel campo della sicurezza nucleare e collaborazione ai programmi internazionali per il nucleare di IV Generazione.
Linea: Collaborazione ai programmi internazionali per il nucleare di IV Generazione
Obiettivo: Progettazione di sistema e analisi di sicurezza
Responsabile del Progetto: Mariano Tarantino, ENEA

Titolo

PRE-TEST CFD ANALYSIS OF THE BLOCKAGE FUEL PIN SIMULATOR (BFPS) TEST SECTION FOR THE NACIE-UP FACILITY

Descrittori

Tipologia del documento: **Rapporto Tecnico**

Collocazione contrattuale: Accordo di programma ENEA-MSE su sicurezza nucleare e reattori di IV generazione

Argomenti trattati:

Generation IV reactors, Tecnologia dei metalli liquidi

Sommario

The present report is focused on the CFD pre-test analysis and design of the new experimental facility 'Blocked' Fuel Pin bundle Simulator (BFPS) that will be installed into the NACIE-UP (NAtural CIrculation Experiment-UPgrade) facility located at the ENEA Brasimone Research Center (Italy).

The BFPS test section will be installed into the NACIE-UP loop facility aiming to carry out suitable experiments to fully investigate different flow blockage regimes in a 19 fuel pin bundle providing experimental data in support of the development of the ALFRED (Advanced Lead-cooled Fast Reactor European Demonstrator) LFR DEMO. In particular, the 'Blocked' Fuel Pin bundle Simulator (BFPS) cooled by lead bismuth eutectic (LBE), was conceived with a thermal power of about 250 kW and a uniform wall heat flux up to 0.7 MW/m^2, relevant values for a LFR. It consists of 19 electrical pins placed on a hexagonal lattice with a pitch to diameter ratio of 1.4 and a diameter of 10 mm.

The geometrical domain of the fuel pin bundle simulator was designed to reproduce the geometrical features of ALFRED, e.g. the external wrapper in the active region and the spacer grids. Pre-tests calculations were carried out by applying accurate boundary conditions; the conjugate heat transfer in the clad is also considered.

The numerical simulation test matrix covered the envisioned experimental range in terms of mass flow rate; the wall heat flux was imposed in order to have a fixed temperature difference across the BFPS in unblocked conditions.

The blockages investigated are internal blockages of different extensions and in different locations (central sub-channel blockage, corner sub-channel blockage, edge sub-channel blockage, one sector blockage, two sector blockage).

The CFD pre-test analysis allowed also investigating the temperature distribution in the clad to operate the test section safely.

Note

Authors: I. Di Piazza, R. Marinari

Copia n. **In carico a: I. Di Piazza**

2			**NOME**			
			FIRMA			
1			**NOME**			
			FIRMA			
0	**EMISSIONE**	**19/09/2016**	**NOME**	I.Di Piazza	A. Del Nevo	M. Tarantino
			FIRMA			
REV.	**DESCRIZIONE**	**DATA**		**REDAZIONE**	**CONVALIDA**	**APPROVAZIONE**

List of content

1. INTRODUCTION

The root causes of the FA blockage are aggregation of solid matter (oxides), dislodged from its intended location or generated in the coolant, transported inside and along with the coolant's flow; this matter could stop inside the FA (mainly because of its narrow spaces) and interfere with the coolant flowing inside the FA. The main consequence of the blockage is a reduction of the coolant flow rate through the FA. Blockage can be instantaneous (when a large enough piece of material obstructs a portion of the channels of the FA) or time dependent (when the aggregation of solid matter piles up in the channels of the FA). For grid-spaced FAs, an internal blockage is generally located in the first grid and it has a flat-like shape (Schultheiss, 1987). FAs are usually designed with a number of inlets slots to prevent a complete and instantaneous blockage.

Fuel Assembly blockage (total or partial) has been extensively analyzed since the early days of fast reactors. While many of these studies refer to Sodium Fast Reactors, the results may be a starting point for LFRs to. The main focus of these analyses is determining the effects of a blockage on the temperature (cladding and coolant) and pressure (coolant) inside the FA as well as at the outlet of the subassembly, and the optimal detection techniques. Investigations carried out within the LEADER FP7 EU project showed that the maximum clad temperature to avoid long term creep in the Ti15-15 cladding material is 650 °C.

Greef (1979) discussed the temperature noise technique for the detection of local blockages in fast reactor subassemblies of a SFR. The results indicate that blockages appreciably smaller than those predicted to produce boiling should be detectable against a background noise level due to subassembly power tilts, on a time scale giving protection against rapidly developing incidents. For LFR, this technique is difficult to be applied because, due to the high boiling temperature of Lead (~1700°C), boiling does not occur in an internal blockage.

Wey et al. (1982) described the development of a Monte Carlo model capable of generating real time temperature signals from a specified input temperature profile and turbulent velocity field. The model used multi-particle batches which permit calculations simulating heat dissipation processes. Various Sodium Loop experiments are outlined which were used to validate the model in turbulent pipe and jet flows. For the latter, a multistage technique was used which enabled modelling of axial variation of the turbulence field. The technique has also been used to predict temperature signals at the outlet of subassemblies with blockages of various sizes at center and corner positions. A simple assessment of the viability of detecting such blockages with a single centrally located sensor is presented. Hae-Yong Jeong et al. (2014) analyzed the temperature rise across each subassembly in order to detect the formation of a significant size of blockage. With the PFBR blockage detection logic, they generate an alarm signal when the assembly-

wide temperature rise deviates 5 K from the pre-determined value and scram signal for the deviation greater than 10 K. The paper proposed a concept of blockage index (BI) by adopting a kernel function of Gaussian type to take advantage of the thermal-hydraulic information in neighboring subassemblies. With the blockage index, a distance-weighted temperature changes for each subassembly is defined and by combining the blockage index for each subassembly into a core wide map of blockage indices, useful information are gathered to determine whether any blockage is introduced or not at some location of subassembly via an adjustment of the range of influence by performing sensitivity studies on reference distance in advance to select a distance factor which describes the blockage phenomena most correctly for the given subassembly design.

Seung-Hwan Seong et al. (2006) used the LES turbulence model in the ANSYS CFX code for analyzing the temperature fluctuation in the upper plenum. After analyzing the temperature fluctuations in the upper plenum, a basic design requirement was established for the flow blockage detection system through a FFT analysis and a statistical analysis. They concluded that response time of a measuring device was less than 13ms and that it should cover a high temperature range of 1000 K. In addition, the resolution of the thermocouple should be less than 2 K and its location should be within 25 cm from the exit of each assembly.

Nomoto et al (1980) installed thermocouple temperature sensors above the central region of the core in the JOYO experimental sodium fast reactor to monitor the outlet coolant temperature of 115 subassemblies. Subassembly outlet coolant temperature distributions were obtained under various power levels, different main cooling system flowrates, and unequal reactor inlet temperatures from the two cooling loops. In addition, coolant temperature and flowrate distributions at the subassembly outlet measured in a zero power experiment are presented. Maity et al. (2011) carried out thermal hydraulic studies to understand temperature dilution experienced by core-temperature monitoring system of a sodium cooled fast reactor. The three-dimensional computational model is validated against experimental results of a water model. The analysis indicates the maximum possible dilution in fuel and blanket subassemblies to be 2.63 K and 46.84 K, respectively. Shifting of thermocouple positions radially outward by 20 mm with respect to subassembly centers leads to an overall improvement in accuracy of thermocouple readings. It is also seen that subassembly blockage that leads to 7% flow reduction in fuel subassembly and 12% flow reduction in blanket subassembly can be detected effectively by the core-temperature monitoring system.

Di Piazza et al. (2014) carried out a CFD study on fluid flow and heat transfer in the Lead-cooled Fuel Pin Bundle of the ALFRED LFR DEMO. The authors developed a detailed thermo-fluid dynamic analysis at various level of geometrical blockage. In particular the closed hexagonal, grid-spaced fuel assembly of the LFR ALFRED was modeled and computed. While the spacer grids were not included in the model, a conservative analysis has been carried out based on the current main geometrical and physical features. Results indicate that critical conditions, with clad temperatures ≈ 900°C, are reached with

geometrical blockage larger than 30% in terms of area fraction. The results show that two main effects can be distinguished: a local effect in the wake/recirculation region downstream the blockage and a global effect due to the lower mass flow rate in the blocked subchannels; the former effect gives rise to a temperature peak behind the blockage and it is dominant for large blockages (>20 %), while the latter effect determines a temperature peak at the end of the active region and it is dominant for small blockages (<10 %). The blockage area was placed at the beginning of the active region, in such a way that both abovementioned phenomena can be seen. Different mass flow rates and different levels of geometrical blockage were imposed from preliminary system code simulations. Transient analyses with fully resolved SST-omega turbulence model were carried out and results indicate that a blockage of ~15 % (in terms of blocked area) leads to a maximum clad temperature around 800°C, and this condition is reached in a characteristic time of 3–4 s without overshoot. Local clad temperatures around 1000°C can be reached for blockages of 30 % or more. CFD simulations indicate that blockages (in terms of blocked area) greater than 15 % could be detected by placing thermocouples in properly selected locations in the plenum region of the FA. Kirsch (1975) presented experimental and theoretical investigations of the flow and temperature distribution in local recirculating flows in rod bundles, downstream of a blockage. A mean coolant temperature in this recirculation zone can be calculated from the dimension of the recirculation zone and the mass exchange rate with the main flow. Similarity analysis for recirculating flow in a simple geometry without rods shows that with a sufficiently high Reynolds number, similar geometry and similar heat distribution, the dimensionless temperature fields in recirculating flows are equal and independent of the Reynolds and Prandtl numbers. This result is also observed to be true for rod bundles, justifying temperature distribution measurements to be performed with water instead of sodium.

2. THE UPGRADE OF THE NACIE FACILITY (NACIE-UP): AN OVERVIEW

The results of the flow blockage simulations presented in this paper will be used to select the location of the thermocouples and other probes in the experiments carried out by a proper BFPS test section installed in the NACIE-UP facility.

NACIE-UP is a rectangular loop which allows to perform experimental campaigns in the field of the thermal-hydraulics, fluid-dynamics, chemistry control, corrosion protection and heat transfer and to obtain correlations essential for the design of nuclear power plant cooled by heavy liquid metals. It basically consists of two vertical pipes of O.D. 2.5 in. (63.5 mm)), working as riser and downcomer, connected by two horizontal pipes of O.D. 2.5 in. (63.5 mm)). The whole height of the facility is about 7.7 m, while the horizontal length is about 2.4 m. A section of the facility is devoted to place the prototypical fuel pin bundle simulator (FPS) test sections in the lower part of the riser. In the last experimental campaign (2015), a wire-wrapped 19-pin 250 kW FPS was mounted. The test section for the blockage experiment will be placed in place of the previous one. A proper heat exchanger is placed in the upper part of the downcomer.

NACIE-UP is made of stainless steel (AISI 304) and can use both lead and the eutectic alloy LBE as working fluid (about 2000 kg, 200 l of total capacity). It was designed to work up to 550°C and 10 bar. The difference in height between the center of the heating section and the center of the heat exchanger is about 5.5 m and it is very important for the amount of the natural circulation. In the riser, an argon gas injection device ensures a driving force to sustain forced convection in the loop.

The P&ID of the facility is reported in Figure 1, while a schematic layout of the primary circuit is reported in Figure 2. The facility includes:

- The Primary side filled with LBE, with 2.5 in. (63.5 mm) pipes. It consists of two vertical pipes, working as riser and downcomer, two horizontal pipes and an expansion tank;
- A Fuel Pin Simulator (19-pins) 250 kW maximum power, placed in the bottom of the riser of the primary side (it will be replaced by the new BFPS test section);
- A Shell and tube HX with two sections, operating at low power (5-50 kW) and high power (50-250 kW). It is placed in the higher part of the downcomer;
- A high mass flow rate induction flow meter (3-15 kg/s) FM102, located in the downcomer, after the HX;
- 3 bubble tubes to measure the pressure drops across the main components and the pipes;
- A differential pressure transducer (1 mbar accuracy) for the test section;
- A prototypical thermal flow meter (ENEA/Thermocoax R&D) based on the heat transfer phenomena across the component;

- Several bulk thermocouples to monitor the temperature along the flow path in the loop;
- The Secondary side, filled with water at 16 bar, connected to the HX, shell side. It includes a pump, a pre-heater, an air-cooler, by-pass and isolation valves, and a pressurizer with cover gas;
- An ancillary gas system, to ensure a proper cover gas in the expansion tank, and to provide gas-lift enhanced circulation;
- A LBE draining section, with 0.5 in. (12.7 mm) pipes, isolation valves and a storage tank.

The ancillary gas system has the function to ensure the cover gas in the expansion tank and to manage the gas-lift system in the riser for enhanced circulation regime.

The primary system is ordinary filled with liquid LBE and it is made by several components, pipes and coupling flanges. Pipes T101, T102, T103, T104, T105 are austenitic SS AISI304 2.5”S40, I.D. 62.68 *mm*. Figure 3 shows a picture of the primary side of the NACIE-UP facility.

An expansion tank (S101) is located at the end of the riser and is partially filled with Argon as cover gas to control the pressure inside the primary circuit. Two level sensors LD101, LD102, are located respectively 80 and 180 *mm* above the outlet nozzle of the riser, inside the expansion vessel.

A drawing of the expansion vessel (S101) is reported in Figure 4. Pipe 1 in Figure 4 is welded to the pipe working as riser (T103) and ends with a nozzle 285 *mm* long inside the tank.

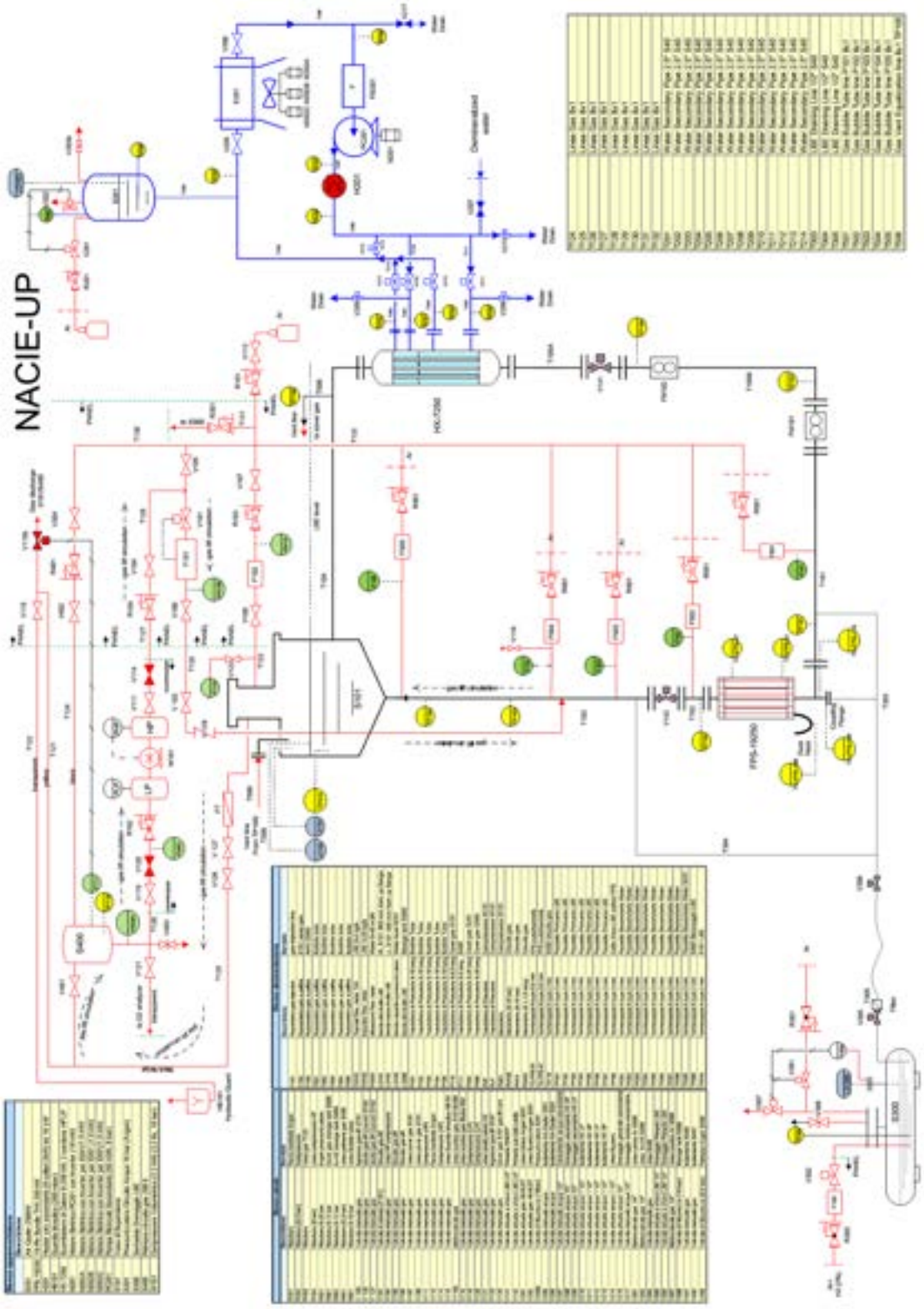

Figure 1: Piping and Instrumentation Diagram (P&ID) of the NACIE-UP facility.

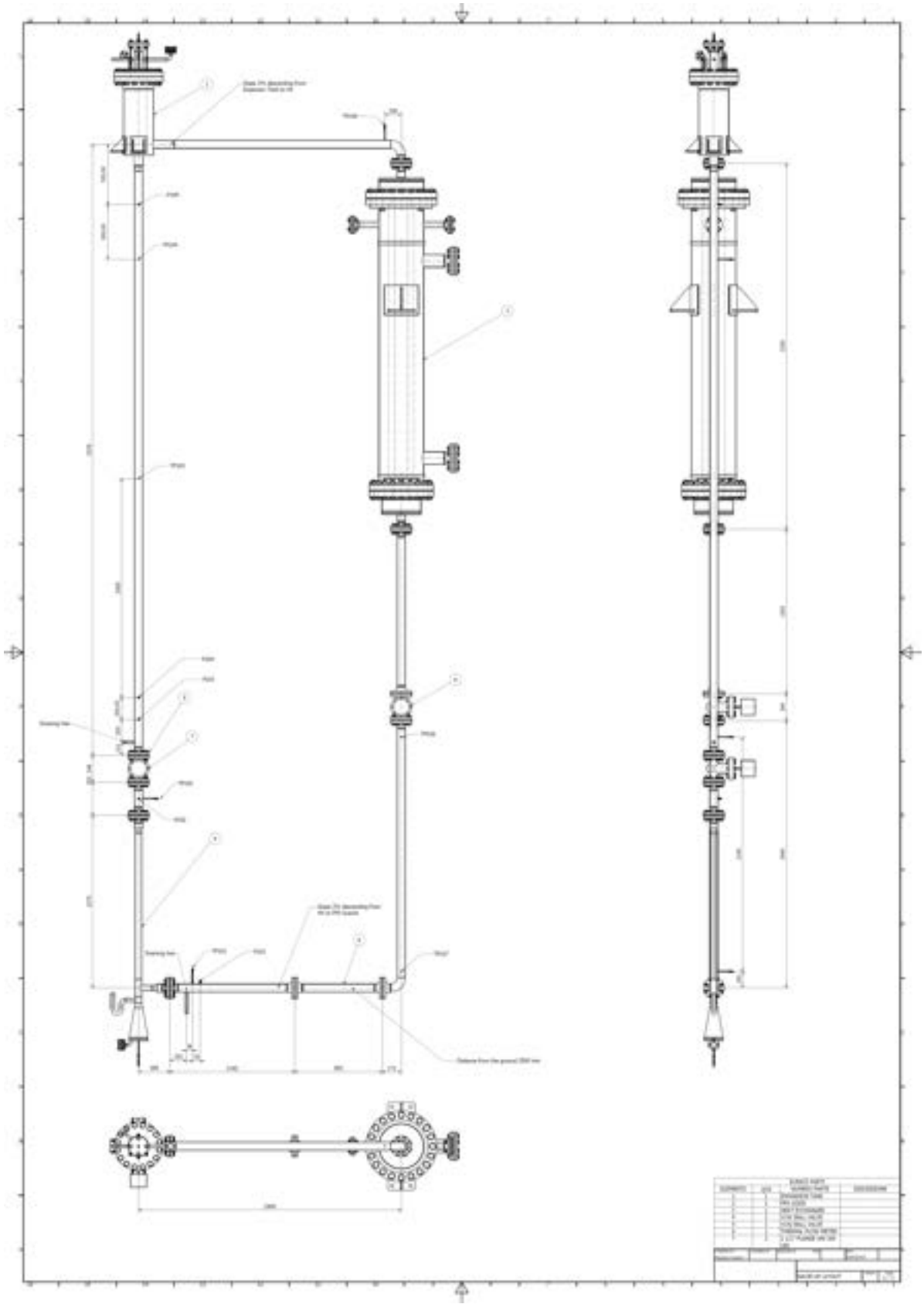

Figure 2: Schematic layout of the NACIE-UP facility.

Figure 3: NACIE-UP facility.

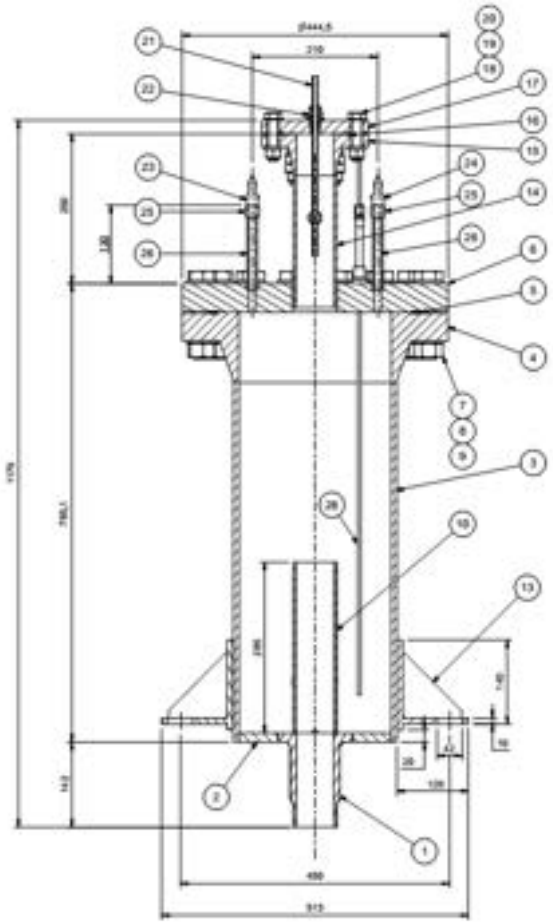

Figure 4: Layout of the expansion vessel inside the primary circuit of the NACIE-UP facility.

The fill and drain system has been designed to be completely controlled by DACS by proper fill and drain operational procedures. This system is made of austenitic SS AISI304 1/2" pipes, isolation valves, a filter (T305) and a storage tank (S300). In Figure 5 some components of the fill and drain system are shown.

Figure 5: Sketches of the fill and drain system of the NACIE-UP facility.

In the riser, an argon gas injection device ensures a driving force to sustain enhanced circulation regime in the loop. The gas injection system is composed of a 9 *mm* I.D. pipe inserted inside the riser and is connected to the ancillary gas system. The pipe is 6135 mm long starting from the 2 ½" coupling flange in the upper part expansion tank and ends with a 4.35 *mm* I.D. hook-shaped pipe.

The secondary side is a 16 *bar* pressurized water loop, with a circulation pump PC201, a pre-heater H201, the HX shell side, an air-cooler E201 and a pressurizer S201. Components of the secondary side are depicted in Figure 6. The pressurizer is connected to the gas lines to ensure an Argon cover gas and to regulate the loop pressure though DACS. Most of the valves are motorized in order to ensure the full operability of the secondary loop by DACS. The valve system allows to drain and fill the two sections of the HX shell separately from the control room. A bypass of the HX is ensured by V214 for the pre-heating of the secondary water. The heating section H201 allows to heat-up the secondary fluid to have flexibility in managing low FPS powers. The ultrasonic flow meter FM201 allows to monitor

the secondary water mass flow rate, while several thermocouples will monitor temperature in the loop; the combination of the two information will allow to quantify the power exchange in the HX. The heat exchanger is shell and tube type and has been designed to exchange heat up to 250 *kW*. Two separated shell sections have been built: a counter-current high-power section (0-30 *kW*) and a cross-flow low power section (30-250 *kW*), both connected to the pressurized water secondary side. The two sections can be drained and filled separately.

Figure 6: Components of the secondary side of the NACIE-UP facility.

3. THE BFPS TEST SECTION

The Blockage Fuel Pin Simulator (BFPS) test section was designed in order to study the local and bulk effects of an internal blockage in a 19-pin LFR ALFRED DEMO-like FPS.
The heat source will consist of 19 electrical pins with an active length L_{active} = 600 mm (L_{total} = 2000 mm, including the *non-active* length) and a diameter *D*= 10 mm. The pitch to diameter ratio is P/D=1.4. The maximum external wall pin heat flux will be ≈0.7 MW/m^2. The pins will be placed on a hexagonal layout by a suitable wrapper, while two grids will maintain the pin bundle in the correct position, the total power of the pin fuel bundle is ≈ 250 kW.
The goals of the experimental campaigns planned on the NACIE-UP loop facility with the BFPS bundle are:

- measurement of the pin wall temperature both with and without blockage by embedded thermocouples;
- measurement of the subchannel temperature;
- Heat Transfer Coefficient (HTC) evaluation;
- axial temperature profiles in the wrapper and in the subchannels;
- check the presence of hot spots and localized peak of temperature;
- evaluation of the thermal mixing above the pin bundle (BFPS);

A drawing of the BFPS test section is shown in Figure 7. A spacer grid is located at the beginning of the active region where the coupling flange is present. Without blockage, the test section allows to characterize the flow and the heat transfer in the FA. By opening the coupling flange located upstream the active region and by closing grid subchannels by caps, proper blockages at the beginning of the active region can be achieved.
The test section is instrumented with 100 thermocouples. The location of the thermocouples in the system was according to the results of the present pre-test analysis.

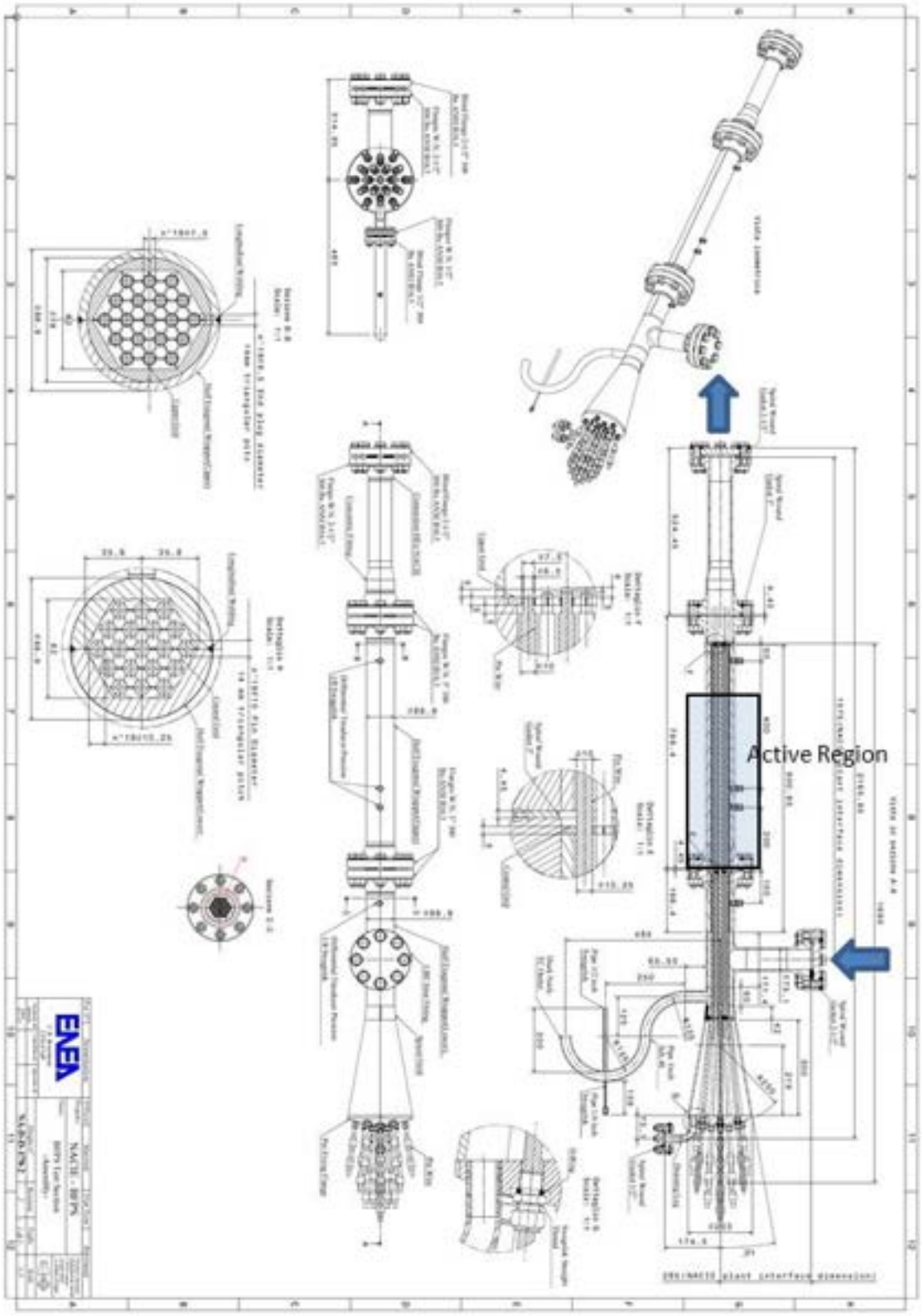

Figure 7 Technical drawing of the BFPS test section.

4. PRE-TEST ANALYSIS

For the CFD pre-test analysis of the BFPS experiment, the test section was modelled. A sketch of the computational domain is reported in Figure 8. It includes (from bottom to top) the developing region, the active region, and the mixing region downstream the FA. The conjugate heat transfer in the hexagonal wrapper and in the coupling flange was also considered. The importance of the conjugate heat transfer in this kind of test sections was definitely assessed in previous works, see Di Piazza (2015) and Doolaard (2015). Constant mass flow rate, temperature at inlet and pressure at outlet were applied for the simulations. The external surface of the hexagonal wrapper is considered adiabatic, being insulated with 100 mm of thermal insulator.

The general purpose code ANSYS CFX 15 was used for all the numerical simulations presented in this paper. The code employs a coupled technique, which simultaneously solves all the transport equations in the whole domain through a false time-step algorithm. The linearized system of equations is preconditioned in order to reduce all the eigenvalues to the same order of magnitude.

The SST (shear stress transport) k–ω model by Menter (1994) was extensively used in this paper. It is formulated to solve the viscous sub-layer explicitly, and requires several computational grid points inside the viscous sub-layer. The turbulent Prandtl number was set to 1.5, according to the literature suggestions (Cheng and Tak, 2006).

Four meshes have been tested to perform a mesh independence analysis, with 10, 15, 19, 24 M nodes on the whole domain and y^+=1 for all the computational grids, see Table 1. Because the results for fluid flow, heat transfer and temperature (maximum and at outlet) of the unblocked case were comparable to a very high degree among the 4 meshes , the mesh C with 19 M nodes was selected representing a good compromise between computational requirements and numerical precision. Two views of mesh C are shown in Figure 9.

Mesh	Mnodes	f Darcy	Nu	$T_{pin,max}$ [°C]
A	10	0.01182	23.86	267.6
B	15	0.01144	17.31	269.8
C	19	0.01130	16.48	272.4
D	24	0.01131	16.52	272.6

Table 1 Mesh adopted for the grid-independence study, with the main overall output parameters.

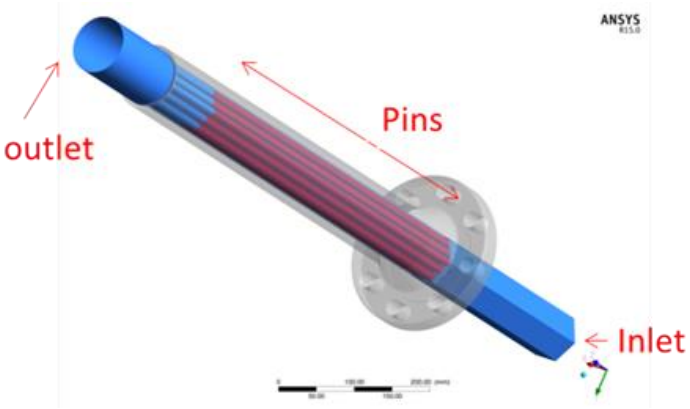

Figure 8 Sketch of the computational domain.

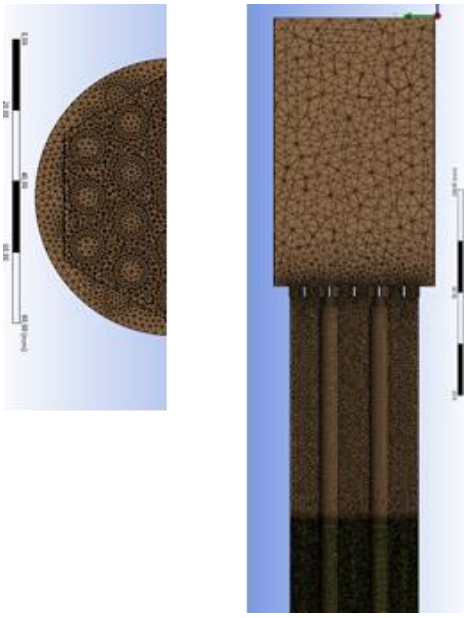

Figure 9 Computational mesh C adopted for the simulations.

Four different blockage types were chosen for the pre-test. These are shown in Figure 10 where type 0 refers to the unblocked case. The mechanical method for implementing the blockage (i.e. how to block the flow in the subchannels) is via a stainless steel cap fixed to the grid spacer, properly fitted according to the type and location of the blockage. A pre-test matrix was prepared for defining the different of blockage types at different mass flow rates. In the test cases presented here, the mass flow rate was kept constant at 16 kg/s, corresponding to 108 kg/s in the ALFRED FA (75% of the nominal flow rate), and it is the maximum flow rate achievable in the NACIE-UP facility. The power of the FPS was 94.2 kW to have an inlet-outlet temperature increase of 40°C. The inlet temperature is 200°C, because at that value the test section is protected from damages during the experiments.

Only the most relevant cases of the complete computational test matrix are presented here, and are summarized in Table 2.

Case	Blockage type	Mass flow rate [kg/s]	Power [kW]	Inlet Temperature [°C]
0	0	16	94.2	200
1	1	16	94.2	200
2	2	16	94.2	200
3	3	16	94.2	200
4	4	16	94.2	200
5	5	16	94.2	200

Table 2 Test matrix presented in the paper.

The mass flow rate was kept constant at the different degree of blockage. This is justified by the fact that in the real ALFRED FA geometry, blockage degrees up to 30% would not affect significantly the flow rate (Di Piazza, 2014).

Figure 11 shows the clad temperature distribution in the active region for the unblocked case 0. The temperature gradient is basically axial as expected with a maximum temperature of the cladding is 261°C. Figure 12 shows the clad temperature distribution in the region behind the blockage for blockage type 1 (sector blockage, case 1). A local temperature peak in the region 100 mm behind the blockage is clearly visible with a maximum temperature of ≈360°C, well above the maximum temperature of the unblocked case. The local temperature increase due to the blockage is ≈150°C. As evidenced in other computational and theoretical studies (Di Piazza, 2015) (Kirsch, 1975) (Roelofs, 2012), the reason for the local temperature peak is the vortex generated downstream by the obstacle represented by the blockage; in the central, stagnation point of the vortex heat is exchanged only by conduction and the temperature increases. This hydrodynamic effect is shown in Figure 13, where temperature field (left) and secondary flow field (right) are shown at the cross-sections at z=10, 20, 30, 45 mm from the blockage (located at z=0 mm at the beginning of the active region, first grid) for case 1 (sector blockage). A shear vortex due to the blockage obstacle is clearly evidenced between z=10 mm and 45 mm with a maximum of the secondary flow. The temperature field shows a peak value in planes *z*= 20, 30 mm where the transversal flow is minimal.

Figure 14 shows the temperature distribution for case 0 (unblocked) and 1 (sector blockage) at the outlet section in the mixing region; please note that the color scales adopted are different for the two graphs. In the unblocked case, mixing guarantees a maximum spatial difference of temperature of ≈1.5°C, while in the blocked case the spatial temperature distribution clearly shows the location of the underlying blockage with a temperature difference of ≈15 °C. The substantial difference both in the value of the temperature in a specific location as well as in the spatial distribution of the temperature confirms the possibility to detect the internal blockage at this level of blockage by putting thermocouples in properly selected locations of the mixing region of the FA.

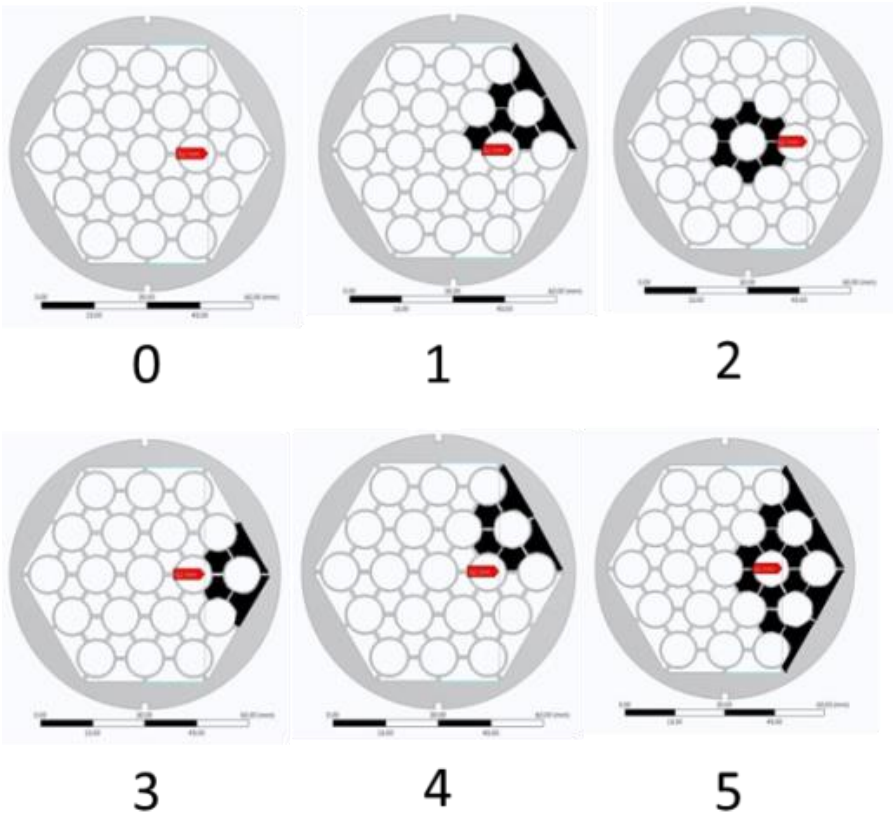

Figure 10 Different blockage types: (0) unblocked; (1) sector; (2) central; (3) corner; (4) edge; (5) two sectors. Subchannels are blocked with a stainless steel caps fixed to the grid spacer (in gray).

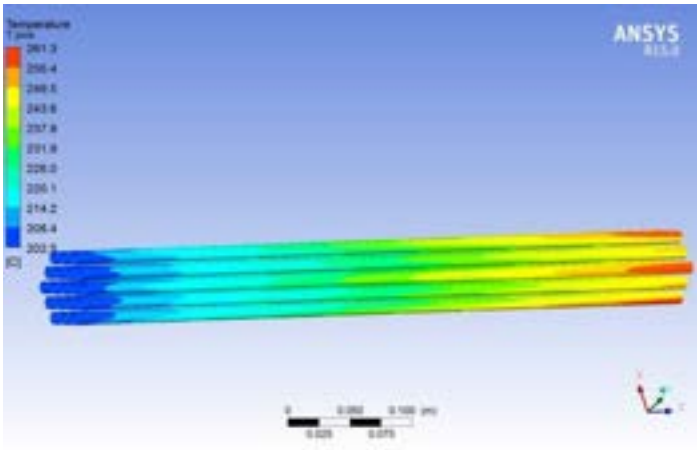

Figure 11 Pin clad temperature field in the unblocked case.

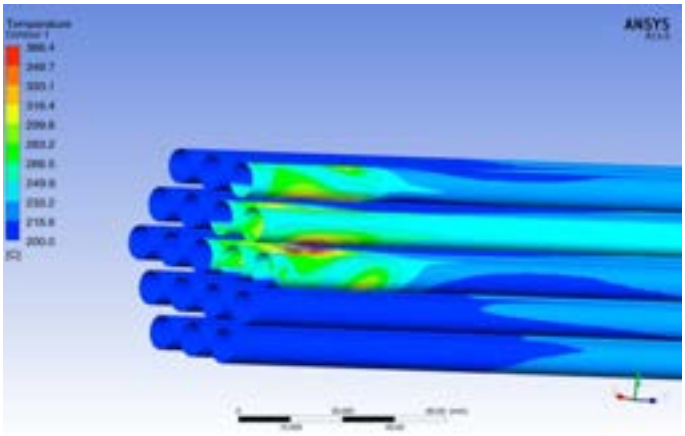

Figure 12 Clad temperature field in the region behind the blockage (blockage type 1).

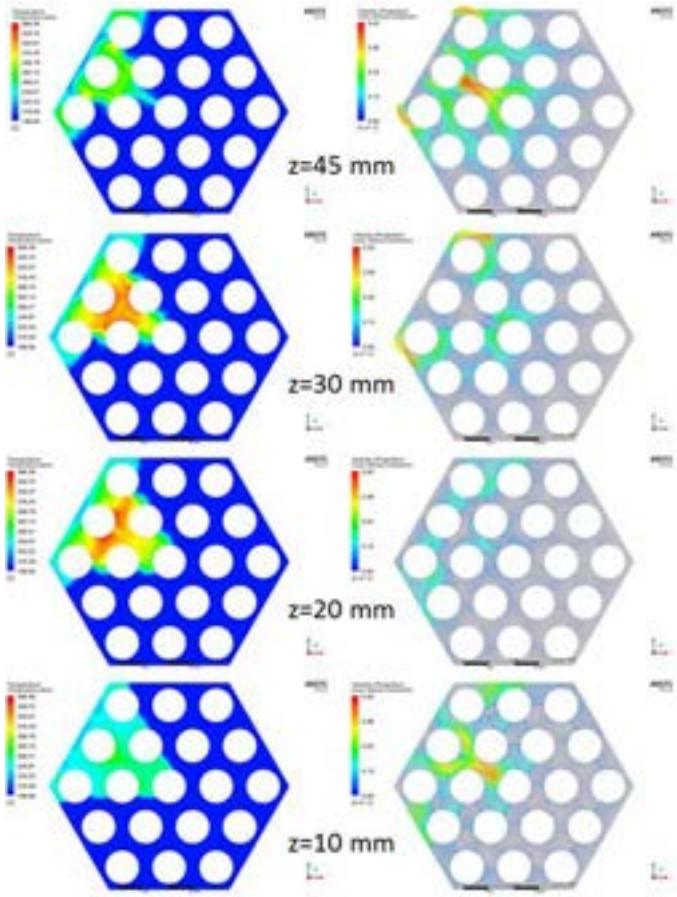

Figure 13 Temperature field (left) and secondary vector plot in four different planes located at z=10, 20, 30, 40, 45 mm from the beginning of the active region.

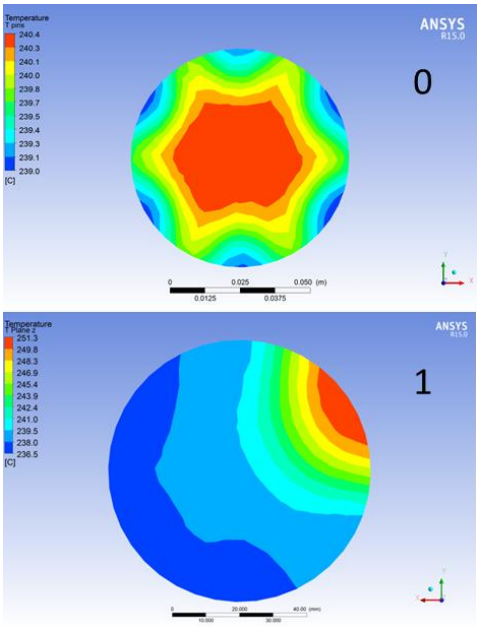

Figure 14 Temperature distribution in the outlet section of the mixing region for case 0 (unblocked) and 1 (sector blockage).

Figure 15 shows the maximum temperature profiles along the streamwise axial direction for all simulated cases, with the axial distance starting from the beginning of the active region. Most of the cases have a similar maximum temperature behind the blockage around 360°C, with a local temperature difference with respect to the unblocked case of ≈150°C. The region of influence behind the blockage is limited to ≈50-100 mm in most cases, and 200 mm for the larger 2 sector blockage (case 5). This result is in line with previous studies (Di Piazza, 2015) (Kirsch, 1975) and the region of influence is tied to the extension of the blocked area. Typically an elongated recirculation vortex of aspect ratio 2-3 behind the blockage is present. A larger blockage will lead to a longer vortex and to a larger region of influence.

The present results suggest the position of the instrumentation in the test section. The blocked region will be monitored with 0.35mm wall-embedded thermocouples, most of them located on the hottest pins in the region of influence. The remaining thermocouples are positioned in order to measure bulk and wall temperatures in the different subchannels and to characterize heat transfer in different conditions. The generic section of the FPS was divided in 36 subchannels, see Figure 16, corresponding to the grid passages at the beginning of the active region, cfr. Figure 10. The bundle was divided in 6 sectors from A to F. The code identifying the subchannel, e.g. B2, refers to the sector (e.g. letter ‘B’) and to the rank (e.g. number ‘2’).

The thermocouples locations are shown in Figure 17, with the instrumented pins colored in red. Pins 1, 2, 5, 15 will be equipped with wall embedded thermocouples on a generatrix parallel to the pin axis, and sub-channel B2 will be instrumented with 0.5 mm bulk thermocouple. The diameter of the wall embedded thermocouples is 0.35 mm.

Sixteen different levels will be considered for the four generatrices and the sub-channel: *z*= 10, 20, 30, 40, 50, 60, 70, 80, 90, 100, 150, 200, 300, 400, 500, 600 mm starting from the beginning of the active region of the pins. Plane at z= 550 mm will be instrumented as in the following to characterize the heat transfer in the unblocked case:

- pins 1, 2, 4, 5, 7, 9, 14, 15 will be instrumented with wall embedded thermocouples;
- sub-channels B1, B2, B5, E1, E5 and the corner sub-channels across B5/C4 and E5/F4 will be instrumented with bulk thermocouples 0.5 mm thickness placed at the center of the subchannel;
- An additional bulk thermocouple of 0.35 mm thickness is placed in subchannel B1 at a distance of 1 mm from the wall.

This instrumentation will allow to collect data on temperature distribution in the case of blockage and to characterize the heat transfer in the unblocked condition by measuring cold spots in the side subchannels and the heat transfer coefficients.

Additional instrumentation (24 **R**esistance **T**emperature **D**etectors) will be placed in the 500 mm mixing region of the test section to collect data for CFD code validation and LBE thermal mixing. RTD will be placed downstream the FPS at different axial, radial and azimuthal positions.

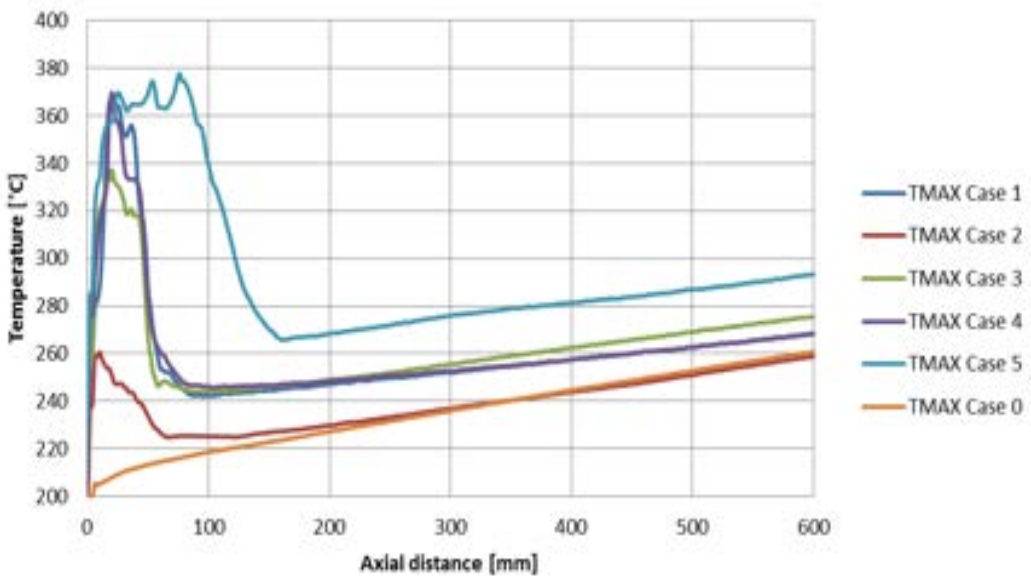

Figure 15 Maximum temperature profile along the streamwise axial direction for the 6 cases investigated.

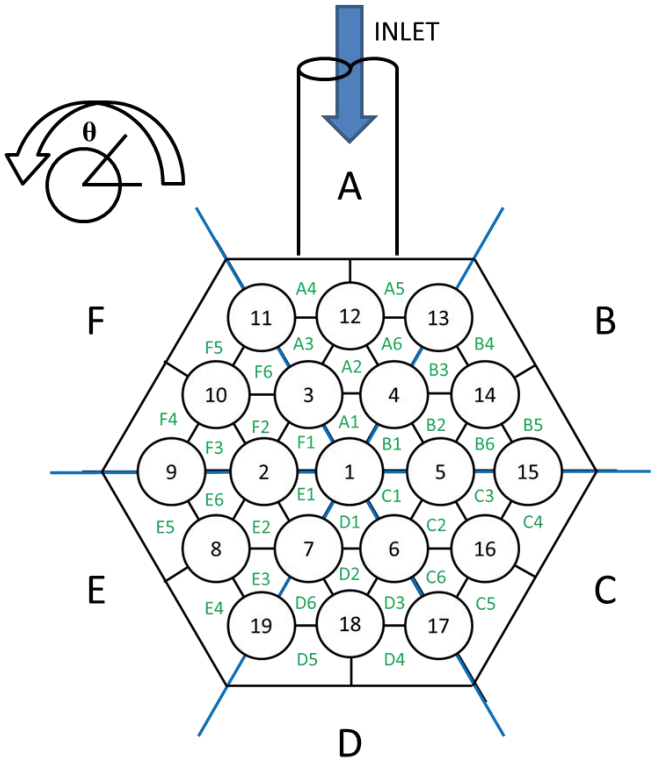

Figure 16 Sketch of a section of the new fuel pin bundle simulator for the NACIE-UP facility as viewed from the top.

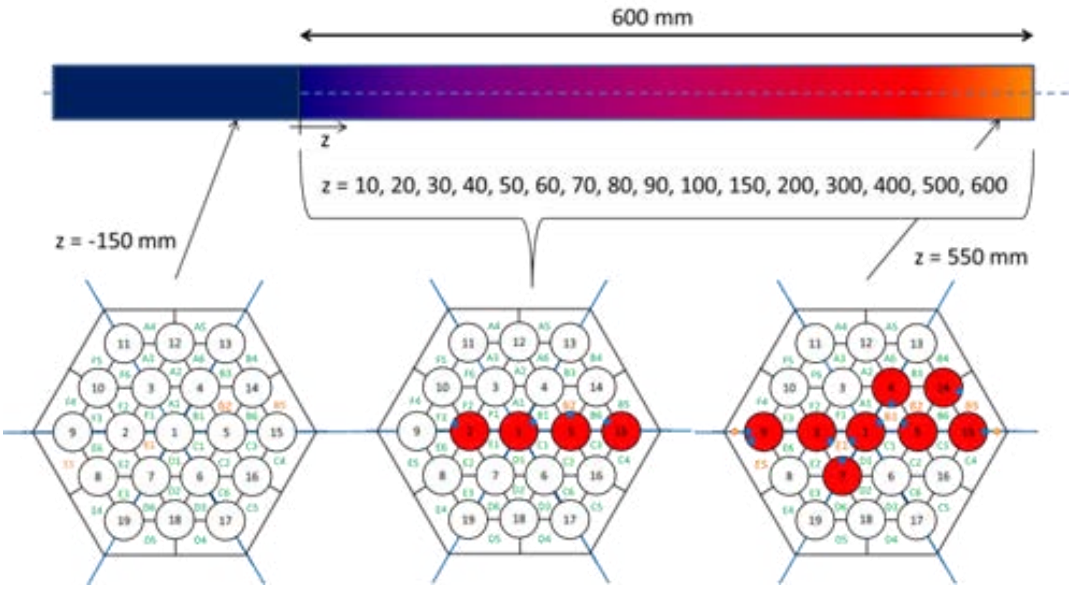

Figure 17 Overall pin bundle TC instrumentation.

5. CONCLUSIONS

The present paper is focused on the CFD pre-test analysis of the 'Blocked' Fuel Pin bundle Simulator (BFPS) that will be installed into the NACIE-UP facility located at the ENEA Brasimone Research Center (Italy).

The BFPS test section will be installed into the existing NACIE-UP loop facility aiming to carry out suitable experiments to fully investigate the effects of different flow blockage regimes in a 19 fuel pin bundle providing experimental data in support of the ALFRED LFR DEMO development. In particular, the fuel pin bundle simulator (BFPS) cooled by lead bismuth eutectic (LBE), was conceived with a thermal power of about 250 kW, an uniform wall heat flux up to 0.7 MW/m^2. It consists of 19 electrical pins placed on a hexagonal lattice with a pitch to diameter ratio of 1.4 and a diameter of 10 mm.

Several blockage types (central, sector, side, corner) were simulated in the grid at the beginning of the active region with a subchannel velocity around 0.8 m/s, relevant for LFR.

Pre-test CFD analysis shows the same basic phenomena of previous studies on larger bundles (Di Piazza, 2014) and documented in literature (Schultheiss, 1987) (Kirsch, 1975). A strong local effect is evident behind the blockage area leading to an elongated vortex with a decrease of heat transfer between the coolant and the cladding. As a consequence, in the region of influence behind the blockage, a temperature rise occurs both for the coolant and for the cladding. The extension of the region of influence is ≈200 mm in the present case, but it scales with the extension of the blockage.

The local overheating is strictly dependent on the operational conditions. For the present case, safe conditions were chosen for the experimental FPS, i.e. 92 kW power with 40°C inlet-outlet temperature rise with an inlet temperature of 200°C.

The local temperature increase due to the blockage is ≈150°C for most of the cases in the present conditions.

The pre-test analysis confirms that blockage could be detected via properly placing the proper instrumentation, (wall-embedded and bulk thermocouples located along the active region, most of them in the region of influence of the blockage). Blockage could be detected placing **R**esistance **T**emperature **D**etectors in the mixing region.

With this instrumentation, the BFPS experiment will provide unique local data on the FA blockage for HLM cooled configurations, will provide a data base for code validation to extend the CFD blockage analysis to a full FA, and it will give indications on the detection methods.

6. REFERENCES

Cheng, X., Tak, N.I., 2006. CFD analysis of thermal-hydraulic behavior of heavy liquid metals in sub-channels. Nucl. Eng. Des. 236, 1874-1885.

Di Piazza, I., Magugliani, F., Tarantino, M., Alemberti, A., 2014. A CFD analysis of flow blockage phenomena in ALFRED LFR demo fuel assembly. Nucl. Eng. Des. 276, 202–215.

Di Piazza, I., Ranieri, M., "CFD PRE-TEST ANALYSIS OF THE FUEL PIN BUNDLE SIMULATOR EXPERIMENT IN THE NACIE-UP HLM FACILITY" 16th International Topical Meeting on Nuclear Reactor Thermal - Hydraulics, NURETH-16, August 30-September 4, 2015, Hyatt Regency Chicago.

Doolaard, H.J., A. Shams, F. Roelofs, K. Van Tichelen, S. Keijers, J. De Ridder, J. Degroote, J. Vierendeels, I. Di Piazza, M. Ranieri, E. Merzari, A. Obabko, P. Fischer "CFD BENCHMARK FOR A HEAVY LIQUID METAL FUEL ASSEMBLY" 16th International Topical Meeting on Nuclear Reactor Thermal - Hydraulics, NURETH-16, August 30-September 4, 2015, Hyatt Regency Chicago.

Greef , C.P., 1979. Temperature fluctuations: An assessment of their use in the detection of fast reactor coolant blockages. Nucl. Eng. Des. 52, 35-55.

Hae-Yong Jeon, Moon-Ghu Park, Seung-Hwan Seon, Jae-Ho Jeong, Effectiveness of Blockage Index for the Detection of Blockage in an SFR Subassembly, Transactions of the Korean Nuclear Society Spring Meeting, Jeju, Korea, May 29-30, 2014.

Kirsch, D., 1975. Investigations on the flow and temperature distribution downstream of local coolant blockages in rod bundle subassemblies. Nucl. Eng. Des. 31, 266-279.

Maity, R.K., Velusamy, K., Selvaraj, P., Chellapandi, P., 2011. Computational fluid dynamic investigations of partial blockage detection by core-temperature monitoring system of a sodium cooled fast reactor. Nucl. Eng. Des. 241, 4994-5008.

Menter, F. R., 1994. Two-Equation Eddy-Viscosity Turbulence Models for Engineering Applications. AIAA Journal 32(8), 1598-1605.

Nomoto, S., Yamamoto, H., Sekiguchi, Y., Tamura, S., 1980. Measurement of subassembly outlet coolant temperature in the JOYO experimental fast reactor. Nucl. Eng. Des. 62, 233–239.

Roelofs, F., Gopala, V.R., Chandra, L., Viellieber, M., Class, A., 2012. Simulating fuel assemblies with low resolution CFD approaches, Nucl. Eng. Des. 250, 548-559.

Schultheiss, G.F., 1987. On local blockage formation in sodium cooled reactors. Nucl. Eng. Des. 100, 427-433.

Seung-Hwan Seong, 2006. Establishment of the design requirements for a flow blockage detection system through a LES analysis of the temperature fluctuation in the upper plenum. Annals of Nuclear Energy 33, 62-70.

Wey, B.O.; Hughes, G.; Overton, R.S, Prediction of temperature fluctuations at the outlet of a blocked subassembly, Proceedings of the L.M.F.B.R. safety topical meeting, 1982.